Asian Journal of Chemistry; Vol. 23, No. 2 (2011), 875-879

ASIAN JOURNAL OF CHEMISTRY

www.asianjournalofchemistry.co.in

Preparation and Characterization of Graphene Oxide Reduced From a Mild Chemical Method

WON-CHUN OH[1,*] and FENG-JUN ZHANG[2]

[1]Department of Advanced Materials & Science Engineering, Hanseo University, Seosan-si, Chungnam-do 356-706, South Korea
[2]Anhui Key Laboratory of Advanced Building Materials, Anhui University of Architecture, Anhui, Hefei 230022, P.R. China

*Corresponding author: Fax: +82 41 6883352; Tel: +82 41 6601337; E-mail: wc_oh@hanseo.ac.kr

(*Received*: 4 June 2010; *Accepted*: 14 October 2010) AJC-9186

Layer structured graphene oxide (GO) was prepared from graphite using the modified Hummers-Offeman method. These layers were comprehensively characterized by X-ray diffraction, Fourier transform infrared spectroscopy, scanning electron microscopy, energy dispersive X-ray analysis, transmission electron microscopy, Raman spectroscopy and atomic force microscopy. FT-IR and EDX measurements indicate the formation of layered structure with strong functional groups of graphene oxide and small partial oxygen containing functional groups were still existed in the sample of reduction of graphene oxide (RGO). From the TEM images, monolayer graphene oxide could be found in a flake form in the graphene oxide and reduction of graphene oxide layers. The intensity ratio between D peak and G peak in the Raman spectra of graphene oxide and reduction of graphene oxide indicated that the as-prepared graphene oxide has a low defect content. Atomic force microscopy results showed that the single layer of graphene oxide has been produced.

Key Words: Graphene oxide, Layer, TEM, Raman, Atomic force microscopy.

INTRODUCTION

Graphene is defined as a flat monolayer of carbon atoms tightly packed into a two-dimensional (2D) honeycomb lattice[1]. Graphene has increasingly attracted attention owing to its fascinating physical properties including the unique electronic[2-9], thermal[10] and mechanical properties[11,12]. These unique properties hold great promise for potential applications in many technological fields such as nanoelectronics, sensors, nanocomposites, batteries, supercapacitors and hydrogen storage[12-15].

All of these engineering applications demand massive production of high quality graphene materials. So far, many methods have been developed to produce graphene. These include micromechanical cleavage[16], epitaxial growth *via* ultra-high vacuum graphitization[17], chemical synthesis through oxidation of graphite[18,19], chemical vapor deposition (CVD) growth of graphene either on a substrate or substrate free[20,21], solvothermal synthesis combined with pyrolysis[22] and liquid phase exfoliation of graphite[23]. These developing techniques to create single layer graphene, which can in general be classified into three different routes: namely (i) mechanical peeling, (ii) epitaxial graphene growth and (iii) solution-based reduction of graphene oxide. Mechanical peeling using the so called "Scotch tape"[16] can only be used to study the fundamental properties of graphene. The epitaxial graphene sheets prepared by treatment of silicon carbide wafers at high temperatures consists of several layers and their overall quality depends highly on the type of substrate materials[24,25]. It is noted that the above two methods are extremely laborious and inefficient and can only produce very small quantities of graphene. The solution-based route has emerged as a promising approach to produce graphene[26,27].

In this solution-based route, graphite oxide is used as a medium to obtain stable graphene dispersion in a solvent. Graphite oxide is a product obtained from oxidation of graphite, which maintains the original layered structure of graphite. Because of the existence of large amounts of hydroxyl, carboxyl, carbonyl and epoxide functional groups attached onto the basal or edge plane, graphite oxide is strongly hydrophilic and easily exfoliated in water, so as to form stable colloidal dispersion. Along with the increase in hydrophilicity during the oxidation process, however, graphite gradually loses its excellent electrical properties and eventually becomes an electrical insulator because the carbon atom is transformed from a planar sp^2-hybridized geometry to a distorted sp^3-hybridized geometry[16]. To recover the electrical conductivity, graphite oxide has to be reduced to remove most of the oxygen-containing functionalities so that the aromatic graphene networks are restored. The reduction process of graphite oxide results gradually the decrease in hydrophilic character, which often leads to irreversible agglomeration and precipitation. To solve the problems of agglomeration and precipitation, a simple and efficient method was also proposed to achieve the reduction of graphite

oxide with hydrazine and ultrasonication. The prepared graphene is stable in aqueous solution, ready to be isolated as monolayer or multilayer graphene.

EXPERIMENTAL

Preparation of graphene oxide: Graphite (KS-6) was selected as the starting material. Graphene oxide (GO) was prepared from graphite according to the Hummers-Offeman method. In brief, graphite powder (10 g) was dispersed in cold concentrated sulphuric acid (230 mL, 98 wt. %, dry ice bath) and potassium permanganate ($KMnO_4$, 30 g) gradually added with continuous vigorous stirring and cooling to prevent the temperature from exceeding 293 K. The dry ice bath was removed and replaced by a water bath and the mixture heated to 308 K for 0.5 h with gas release under continuous stirring, followed by slow addition of deionized water (460 mL), which produced a rapid increase in solution temperature up to a maximum of 371 K. The reaction was maintained for 40 min in order to increase the oxidation degree of the graphene oxide product and then the resultant bright-yellow suspension was terminated by addition of more distilled water (140 mL) followed by hydrogen peroxide solution (H_2O_2, 30 %, 30 mL). The solid product was separated by centrifugation at 3000 rpm and washed initially with 5 % HCl until sulphate ions were no longer detectable with barium chloride and then washed three times with acetone and air dried overnight at 338 K.

Reduction of graphene oxide: Reduction of graphene oxide was performed as follows: Twenty-five milligrams of the graphene oxide powder was placed in a cup and 200 mL de-ionized water was then added. Ten minutes of magnetic stirring at 200 rpm yielded an inhomogeneous brown suspension. The resulting suspensions were further treated with a reduction agent hydrazine solution (1:5, volume ratio of hydrazine to de-ionized water) under ultrasonication (0.5 h, 1.3×10^5 J) and after dried at 373 K, the sample reduced from graphene oxide (RGO) was produced.

Characterizations of samples: XRD measurements were performed for graphene oxide and reduced graphene oxide samples at room temperature. XRD patterns were obtained with a diffractometer (Shimata XD-D1, Japan) using CuK_α radiation. SEM was used to observe the surface state and structure of the samples using a scanning electron microscope (Jeol, JSM-5200, Japan). EDX spectroscopy was used to measure the elemental analysis of the composites. Raman spectra were utilized to detect the possible structural defects in graphene flakes. The measurements were carried out by a Horiba Jobin Yvon LabRAM using a 100 × objective lens with a 532 nm laser excitation. Thin films (*ca.* 30 nm) were prepared by vacuum filtration of the dispersions through porous alumina membranes. The state of the dispersed graphene was observed using transmission electron microscopy (TEM, Jeol, JEM-2010, Japan). TEM at an acceleration voltage of 200 kV was used to investigate the number and the stacking state of graphene oxide layers on various samples. TEM specimens were prepared by placing a few drops of sample solution on a carbon grid. Fourier transform-infrared (FT-IR) spectroscopy (FTS 3000MX, Biored Co.) was used to characterize the composite materials. The RGO sample was also characterized by atomic force microscopy (AFM, Head mode, frequency 0.803 Hz, Veeco NanoScope IIIa Multimode, DI, USA). Atomic force microscopy observation was conducted for the graphene oxide layers and the samples for AFM analyses were precisely prepared by depositing the hydrosol of graphene oxide on freshly cleaved mica surfaces.

RESULTS AND DISCUSSION

Surface chemistry: The results of the EDX elemental microanalysis of C, O and N elements are listed in Table-1. The C contents of the graphene oxide and reduced graphene oxide are 53.51 and 84.95 %, respectively. It can be expected that the C contents of the reduced graphene oxide in the composites increased due to reduction treatment of partial oxygen containing functional groups. Moreover, the O contents of reduced graphene oxide are only 9.19 % and the mass ratio of O/C is 0.108. It was indicated that some oxygen containing functional groups were still existed in the sample of reduced graphene oxide. The increase in nitrogen contents after reduction most likely originated from the reactions between graphene oxide and the reducing agent[27-29], which are schematically shown in Fig. 1. Hydrazine readily reacted with the epoxide functional groups to form the hydrazine alcohols, which were mainly responsible for the incorporation of nitrogen.

TABLE-1
EDX ELEMENTAL MICROANALYSIS OF C, O AND N ELEMENTS

Material	Elements (wt. %)			
	C	O	N	O/C ratio
GO	53.51	44.65	–	0.834
RGO	84.95	9.19	2.49	0.108

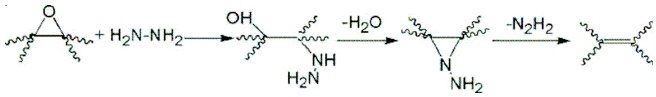

Fig. 1. Proposed reaction pathway for epoxide reduction with hydrazine

Fig. 2 illustrates the FT-IR spectra of the powdery graphene oxide and reduced graphene oxide. The most characteristic features in the FT-IR spectrum of graphene oxide are the adsorption bands corresponding to the C=O carbonyl stretching at 1728 cm^{-1} and the C-O stretching at 1050 cm^{-1} [30,31]. The

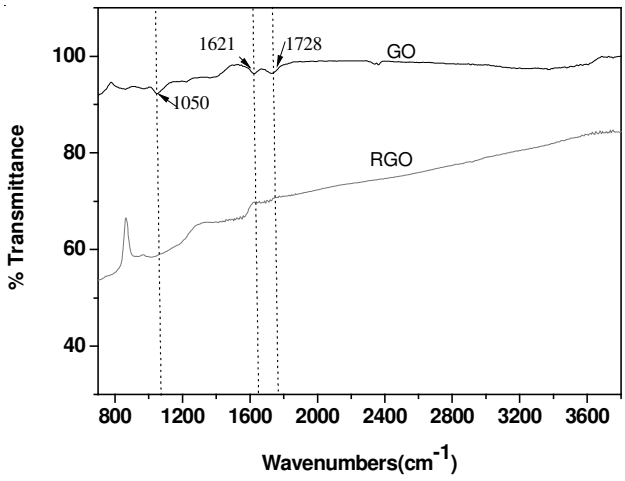

(a)

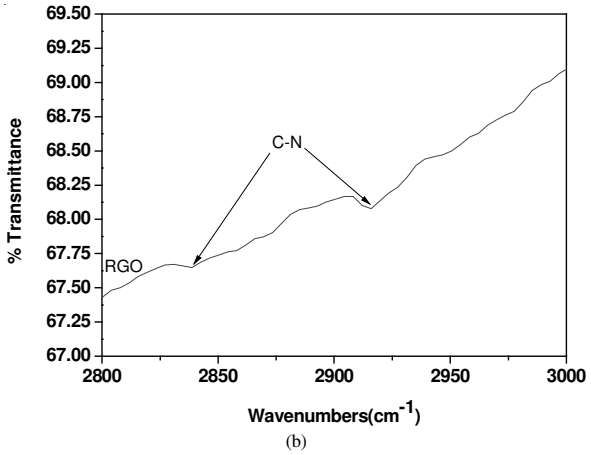

Fig. 2. (a) FTIR spectra of GO and RGO; (b) the magnified C-N stretch vibration in the spectrum of RGO

broad band at 3400 cm^{-1} is due to the stretching vibrations of structural OH groups, the resonance at 1621 cm^{-1} can be assigned to the vibrations of the adsorbed water molecules. But they may also contain components from the skeletal vibrations of un-oxidized graphitic domains[30,32,33]. However, these peaks in the spectrum of reduced graphene oxide almost totally disappear, suggesting that all oxygen-containing functional groups in reduced graphene oxide layers are nearly completely removed during the reduction treatment. Nevertheless, two weak, but sharp peaks turned up within the range of 2920-2850 cm^{-1} corresponding to C-N stretch vibration was found in the Fig. 1(b), which is consistent with the EDX analysis (Table-1).

Structural properties: The structural properties of powdery graphene oxide and reduced graphene oxide were characterized using the XRD analysis, as shown in Fig. 3. The characteristic 2θ peak of graphene oxide appeared at 10.34° corresponds to a d-spacing of approximately 8.546 Å that is consistent with the interlayer space of graphene oxide sheets reported in the literatures, due to the existence of oxygen-rich groups on both sides of the sheets and water molecules trapped between the sheets[30,31]. The XRD pattern of reduced graphene oxide shows a distinct peak at 11.07° corresponding to a d-spacing of 7.984 Å, which might attribute to the stacking of graphene oxide layers by ultrasonic treatment.

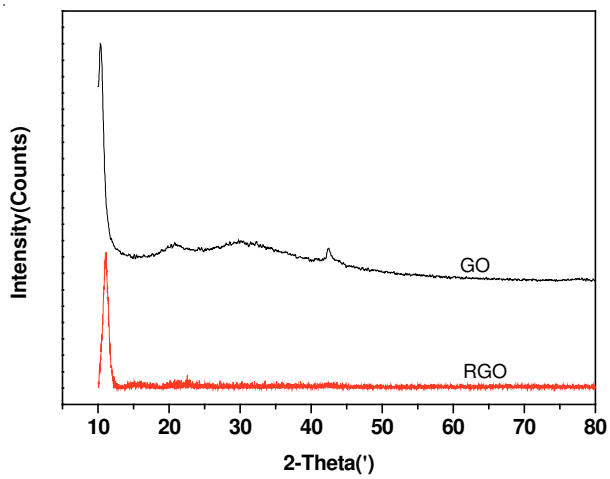

Fig. 3. XRD patterns of graphene oxide and reduced graphene oxide

Degree of exfoliation and thickness of reduced graphene oxide: Raman spectroscopy is a non-destructive technique to characterize graphite materials, in particular to determine the defects and the ordered and disordered structures of graphene. Fig. 4 shows the Raman spectra of the powdery GO and RGO. The Raman spectra of powdery GO displays two prominent peaks at 1356 and 1596 cm^{-1}, corresponding to the well-documented D- and G-band. The Raman spectra of the obtained RGO also show both D- and G-bands at 1347 and 1596 cm^{-1} with comparable D/G intensity ratios to that of powdery GO, which suggests that the skeleton structure of GO remains in the RGO. The G line represents the in-plane bond stretching motion of the pairs of C sp^2 atoms (the E_{2g} phonons); while the D line corresponds to breathing modes of rings or j-point phonons of A_{1g} symmetry[23]. Usually, the graphene powders synthesized by chemical approach show a strong D band in the Raman spectrum with the intensity ratio of $I_D/I_G > 1$ due to the defects and partially disordered crystal structure of graphene sheets. It is noted here that the intensity of the G band is significantly higher than that of the D band, suggesting that the prepared graphene has low defect content[34,35].

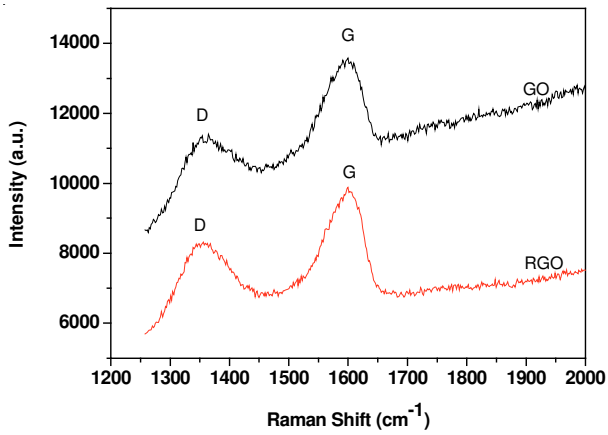

Fig. 4. Raman spectra of graphene oxide and reduced graphene oxide

Fig. 5 shows the SEM images of GO and RGO composites, respectively. The sample shows platelike forms without any amorphous or other kinds of crystallized phase particles. Morphology of GO is observed as flaky texture reflecting its layered microstructure as shown in Fig. 5(a). The larger interspaces of the layer and the thinner layer edges of GO can be clearly seen in Fig. 5(a). RGO composites show a relatively close surface morphology, which may be due to the exfoliation of the GO layers during the ultrasonic treatment process in aqueous media Fig. 5(b).

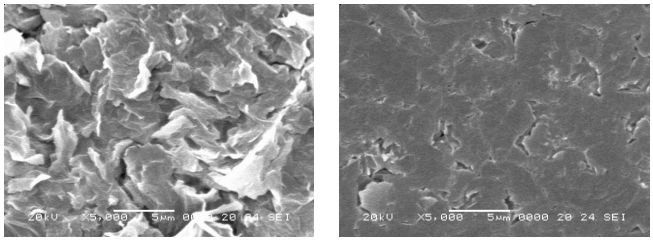

(a) GO (b) RGO

Fig. 5. SEM images of (a) graphene oxide and (b) reduced graphene oxide

TEM images of RGO is compared with that of pristine GO in Fig. 6. The morphology of GO, consisting of thin stacked flakes of shapes and having well defined multilayered structure at the edge, can be clearly seen in Fig. 6(a). It was also clearly seen that monolayer and few-layer graphenes near the edge in the sample of RGO were found [Fig. 6(b)]. The fact that RGO was "dressed" on the surface of GO layers [Fig. 6(b)] may be interpreted by Fig. 3. It was proposed that the electronegativity of oxygen atom of -OH and -COOH groups on GO layer surface facilitated the further oriented aggregation of cation radical of carbon. In addition, the surface oxygen-containing groups of GO might form the H-bond with the carbon atom of RGO.

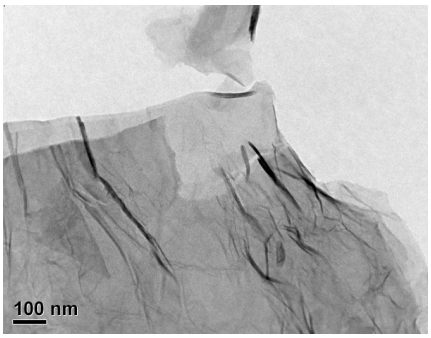

(a) GO

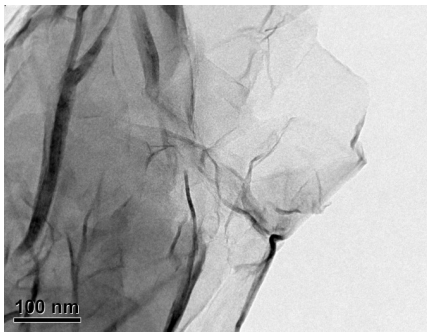

(b) RGO

Fig. 6. TEM images of (a) GO and (b) RGO

AFM was employed to characterize the degree of exfoliation of graphene sheets. As shown in Fig. 7a, a flat graphene sheet was selected for further investigation using the three-dimensional (3D) view. The graphene surface was rough on the nanoscopic scale with some wrinkles, which may be due to (i) the existence of functional groups and (ii) the space resulting from the evaporation of solvent. By line scanning across the plain area of this sheet, as expected, the surface morphologies were quite different. The mean height of the obtained layers is 3.09-9.78 nm. Because of the existing space between the sheets and substrate due to the evaporation of solvent and the limitation of the technique arising from the relatively large curvature radius of the AFM tip, the actual thickness of the graphene sheet was difficult to measure with any accuracy. Nevertheless, the estimation of the height can be viewed as the upper bound of the thickness of the sheet. According to the previous studies on statistical evaluation, the mean thickness of a single graphene sheet is suggested *ca.* 1.0 nm[36]. Given the existence of residual oxygen containing functional groups, the layers should be relatively thicker.

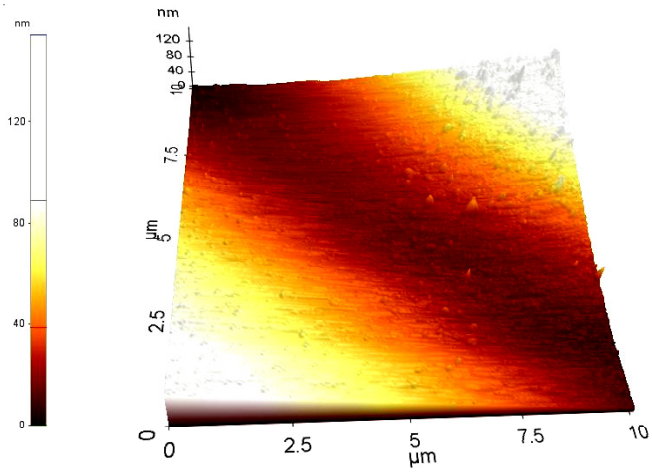

Fig. 7. 3D topography of AFM image of RGO

Conclusion

In this study, thinner layer structured graphene oxide were produced. FT-IR spectroscopy showed that all oxygen-containing functional groups in RGO layers are nearly completely removed. The D peak as well as the G peak witnesses the existence of defect-free monolayer and few-layer graphenes in the sample of RGO. It was also clearly seen that few-layer graphenes were found in the TEM image of RGO. From the result of AFM, the mean height of the obtained RGO layers is 3.09-9.78 nm.

ACKNOWLEDGEMENTS

This work was supported by Research Foundation from Hanseo University in 2010. The authors are grateful to staffs in the University for financial support.

REFERENCES

1. A.K. Geim and K.S. Novoselov, *Nat. Mater.*, **6**, 183 (2007).
2. K.S. Novoselov, A.K. Geim, S.V. Morozov, D. Jiang, M.I. Katsnelson, I.V. Grigorieva, S.V. Dubonos and A.A. Firsov, *Nature*, **438**, 197 (2005).
3. K.S. Novoselov, Z. Jiang, Y. Zhang, S.V. Morozov, H.L. Stormer, U. Zeitler, J.C. Maan, G.S. Boebinger, P. Kim and A.K. Geim, *Science*, **315**, 1379 (2007).
4. C. Gomez-Navarro, R.T. Weitz, A.M. Bittner, M. Scolari, A. Mews, M. Burghard and K. Kern, *Nano. Lett.*, **7**, 3499 (2007).
5. H.B. Heersche, P. Jarillo-Herrero, J.B. Oostinga, L.M.K. Vandersypen and A.F. Morpurgo, *Nature*, **446**, 56 (2007).
6. Y. Kopelevich and P. Esquinazi, *Adv. Mater.*, **19**, 4559 (2007).
7. G.M. Rutter, J.N. Crain, N.P. Guisinger, T. Li, P.N. First and J.A. Stroscio, *Science*, **317**, 219 (2007).
8. N. Tombros, C. Jozsa, M. Popinciuc, H.T. Jonkman and B.J. van Wees, *Nature*, **448**, 571 (2007).
9. J.B. Oostinga, H.B. Heersche, X.L. Liu, A.F. Morpurgo and L.M.K. Vandersypen, *Nat. Mater.*, **7**, 151 (2008).
10. A.A. Balandin, S. Ghosh, W. Bao, I. Calizo, D. Teweldebrhan, F. Miao and C.N. Lau, *Nano. Lett.*, **8**, 902 (2008).
11. D.A. Dikin, S. Stankovich, E.J. Zimney, R.D. Piner, G.H.B. Dommett, G. Evmenenko, S.T. Nguyen and R.S. Ruoff, *Nature*, **448**, 457 (2007).
12. S. Stankovich, D.A. Dikin, G.H.B. Dommett, K.M. Kohlhaas, E.J. Zimney, E.A. Stach, R.D. Piner, S.T. Nguyen and R.S. Ruoff, *Nature*, **442**, 282 (2006).
13. X. Wang, L.J. Zhi and K. Mullen, *Nano. Lett.*, **8**, 323(2008).
14. J.S. Wu, W. Pisula and K. Mullen, *Chem. Rev.*, **107**, 718 (2007).
15. J.H. Chen, M. Ishigami, C. Jang, D.R. Hines, M.S. Fuhrer and E.D. Williams, *Adv. Mater.*, **19**, 3623 (2007).
16. K.S. Novoselov, A.K. Geim, S.V. Morozov, D. Jiang, Y. Zhang and S.V. Dubonos, *Science*, **306**, 666 (2004).

17. C. Berger, Z.M. Song, X.B. Li, X.S. Wu, N. Brown and C. Naud, *Science*, **312**, 1191 (2006).
18. X.L. Li, G.Y. Zhang, X.D. Bai, X.M. Sun, X.R. Wang and H.J. Dai, *Nature Nanotech*., **3**, 538 (2008).
19. V.C. Tung, M.J. Allen, Y. Yang and R.B. Kaner, *Nature Nanotech*., **4**, 25 (2009).
20. K.S. Kim, Y. Zhao, H. Jang, S.Y. Lee, J.M. Kim and K.S. Kim, *Nature*, **457**, 706 (2009).
21. A. Dato, V. Radmilovic, Z. Lee, J. Phillips and M. Frenklach, *Nano. Lett*., **8**, 2012 (2008).
22. M. Choucair, P. Thordarson and J.A. Stride, *Nature Nanotech*., **4**, 30 (2009).
23. M. Lotya, Y. Hernandez, P.J. King, R.J. Smith, V. Nicolosi and L.S. Karlsson, *J. Am .Chem. Soc*., **131**, 3611 (2009).
24. C. Berger, Z. Song, X. Li, X. Wu, N. Brown, C. Naud, D. Mayou, T. Li, J. Hass, A.N. Marchenkov, E.H. Conrad, P.N. First and W.A. Heer, *Science*, **312**, 1191 (2006).
25. P.W. Sutter, J.I. Flege and E.A. Sutter, *Nature Mater*., **7**, 406 (2008).
26. D. Li, M.B. Müller, S. Gilje, R.B. Kaner and G.G. Wallace, *Nat. Nanotech*., **3**, 101 (2008).
27. S. Stankovich, D.A. Dikin, R.D. Piner, K.A. Kohlhaas, A. Kleinhammes, Y. Jia, Y. Wu, S.T. Nguyen and R.S. Ruoff, *Carbon*, **45**, 1558 (2007).
28. H.C. Schniepp, J. Li, M.J. Mcallister, H. Sai, M. Herrera-Alonso, D.H. Adamson, R.K. Prud'homme, R. Car, D.A. Saville and I.A. Aksay, *J. Phys. Chem. B*, **110**, 8535 (2006).
29. Y. Geng, S.J. Wang and J.K. Kim, *J. Colloid. Interf. Sci*., **336**, 592 (2009).
30. T. Szabo, O. Berkesi and I. Dekany, *Carbon*, **43**, 3186 (2005).
31. G.I. Titelman, V. Gelman, S. Bron, R.L. Khalfin and Y. Cohen, *Carbon*, **43**, 641 (2005).
32. M. Mermoux, Y. Chabre and A. Rousseau, *Carbon*, **29**, 469 (1991).
33. S. Stankovich, R.D. Piner, S.T. Nguyen and R.S. Ruoff, *Carbon*, **44**, 3342 (2006).
34. A.C. Ferrari and J. Robertson, *Phys. Rev. B*, **61**, 14095 (2000).
35. G.X. Wang, B. Wang, J.S. Park, Y. Wang, B. Sun and J. Yao, *Carbon*, **47**, 3242 (2009).
36. M.J. McAllister, J. Li, D.H. Adamson, H.C. Schniepp, A.A. Abdala, J. Liu, M. Herrera-Alonso, D.L. Milius, R. Car, R.K. Prud'homme and I.A. Aksay, *Chem. Mater*., **19**, 4396 (2007).